

<https://doi.org/10.1038/s42003-025-07541-x>

# Fasting activates optineurin-mediated mitophagy in chondrocytes to protect against osteoarthritis

Check for updates

Min-Na Zhang<sup>1,5</sup>, Ran Duan<sup>2,5</sup>, Gui-Hong Chen<sup>3</sup>, Mei-Jun Chen<sup>3</sup>, Chun-Gu Hong<sup>4</sup>, Xin Wang<sup>4</sup>, Zhi-Lin Pang<sup>1</sup>, Chun-Yuan Chen<sup>4</sup>, Hua-Feng Liu<sup>3</sup>, Da Zhong<sup>4</sup>✉, Hui Xie<sup>4</sup>✉, Wen-Bao Hu<sup>3</sup>✉ & Zheng-Zhao Liu<sup>3</sup>✉

Mitochondrial homeostasis plays a crucial role in the pathogenesis of osteoarthritis (OA), a chronic musculoskeletal disorder characterized by articular cartilage degeneration and chondrocyte apoptosis. However, molecular mechanisms underlying the association between mitophagy and OA remain unclear. Here, we aimed to investigate the role of the autophagy receptor protein optineurin (OPTN) in OA, and explore the effects of dietary intervention on OA symptoms and its relationship with OPTN-mediated mitophagy. Our findings showed the downregulation of OPTN in patients with OA. Using an *Optn*-knockout mouse model, we demonstrated that OPTN deficiency leads to impaired mitophagy, resulting in the accumulation of damaged mitochondria, increased production of reactive oxygen species, and chondrocyte apoptosis. Furthermore, fasting prevented OA progression by activating OPTN-mediated mitophagy and maintaining mitochondrial homeostasis in mice. The present study revealed a novel mechanism by which OPTN-mediated mitophagy influences chondrocytes and the OA phenotype in *Optn*-knockout mice, suggesting that OPTN-mediated mitophagy plays a crucial role in OA development and progression. This study provides new insights into the pathogenesis of OA and offers a potential avenue for the development of novel drugs targeting OPTN to mitigate OA progression.

Osteoarthritis (OA) is a common chronic musculoskeletal disorder characterized by articular cartilage erosion, subchondral bone formation, synovial inflammation, abnormal angiogenesis, and joint stiffness<sup>1</sup>. The first-line treatment approach for OA includes exercise therapy, weight reduction, patient education, and self-management to enhance the ability of the patient to manage their condition effectively. Surgical referral for knee joint replacement may be considered in patients with end-stage OA<sup>2</sup>. However, no effective treatment methods are available currently, which could be attributed to the lack of understanding of the pathogenesis of OA. In recent years, with the growing number of patients with OA, investigations to identify effective alternative approaches to prevent and treat OA have gained increasing interest. Several classical signaling pathways, including transforming growth factor beta (TGFB), insulin-like growth factor (IGF),

wingless-type MMTV integration site family (WNT), Indian hedgehog (IHH), hypoxia-inducible factor (HIF), fibroblast growth factor (FGF), vascular endothelial growth factor (VEGF), and mammalian target of rapamycin (mTOR), have been implicated in the pathogenesis of OA<sup>1</sup>. Recent studies have demonstrated that OA can be prevented and treated by interfering with autophagy signaling pathways<sup>3,4</sup>.

Autophagy is a cellular mechanism that maintains cell survival under stress conditions. Mitophagy, a type of selective autophagy, plays a crucial role in eliminating impaired mitochondria, preserving optimal mitochondrial functionality, and balancing cellular energy metabolism<sup>5</sup>. Mitophagy has also been shown to contribute to cartilage degeneration in patients with OA<sup>6</sup>. Specifically, insufficient mitophagy leads to cartilage damage in the joints<sup>7</sup>, while increased mitophagy leads to articular cartilage apoptosis<sup>8</sup>.

<sup>1</sup>Department of Sports Medicine, Xiangya Hospital, Central South University, Changsha, 410008 Hunan, China. <sup>2</sup>The First Affiliated Hospital of Chongqing Medical University, Chongqing, 400016 Sichuan, China. <sup>3</sup>Guangdong Provincial Key Laboratory of Autophagy and Major Chronic Non-Communicable Diseases, Key Laboratory of Prevention and Management of Chronic Kidney Disease of Zhanjiang City, Institute of Nephrology, Affiliated Hospital of Guangdong Medical University, Zhanjiang, 524001 Guangdong, China. <sup>4</sup>Department of Orthopedics, Movement System Injury and Repair Research Center, Xiangya Hospital, Central South University, Changsha, 410008 Hunan, China. <sup>5</sup>These authors contributed equally: Min-Na Zhang, Ran Duan. ✉e-mail: [zhongda@csu.edu.cn](mailto:zhongda@csu.edu.cn); [huixie@csu.edu.cn](mailto:huixie@csu.edu.cn); [huwenbao@gdmu.edu.cn](mailto:huwenbao@gdmu.edu.cn); [liuzhengzhao@gdmu.edu.cn](mailto:liuzhengzhao@gdmu.edu.cn)

However, the exact regulatory mechanisms underlying mitophagy in OA remain unclear.

Optineurin (OPTN) is an important receptor that mediates mitophagy<sup>9</sup>. Our previous studies demonstrated that OPTN plays a pivotal role in maintaining balanced bone metabolism<sup>10</sup>. Nevertheless, the association between the bone-protective effects of OPTN and mitophagy is not clear. Fasting activates cellular autophagy by energy restriction and plays a crucial regulatory role in maintaining mitochondrial quality control<sup>11,12</sup>. Fasting has also been shown to alleviate OA<sup>13</sup>; however, the underlying mechanisms remain unclear. Building on these studies, we hypothesized that fasting can activate OPTN-mediated mitophagy in chondrocytes and alleviate OA.

To test this hypothesis, in the present study, we aimed to assess the effects of impaired mitophagy on articular cartilage. Using tissue samples from patients with OA, we confirmed the downregulation of OPTN in patients with OA. Subsequently, we used *Optn*-deficient mice to understand the association between OPTN and mitophagy in OA. Additionally, we tested whether fasting could be used as a lifestyle intervention to promote weight loss and activate OPTN-mediated mitophagy in patients with OA. We show that defects in the autophagy receptor protein OPTN can block mitophagy and induce OA phenotypes. We also show that fasting can effectively increase the expression levels of OPTN and mitophagy, concomitantly improving OA. This study underscores the importance of addressing defects in OPTN and offers valuable therapeutic strategies for OA.

## Results

### Downregulation of OPTN in samples from patients with OA and its importance in OA progression

Our previous study demonstrated that *Optn*-knockout mice exhibited cellular senescence in their bone marrow-derived mesenchymal stem cells and damaged cartilage tissues, indicating an increased risk of osteoporosis in these mice<sup>10</sup>. In this study, immunohistochemical staining for OPTN in diseased and normal tissue samples from 17 patients with OA revealed a remarkable downregulation of OPTN in diseased cartilage tissues compared to that in normal cartilage tissues (Fig. 1a, b). Three-dimensional reconstruction imaging using micro-computed tomography (micro-CT) revealed increased bone formation at the injured site (Fig. 1c), with an increased trabecular bone volume to total volume (Tb.BV/TV) ratio, thickness (Tb.Th), trabecular number (Tb.N), and decreased trabecular separation (Tb.Sp) (Fig. 1d–g).

Next, we investigated whether the downregulation of OPTN expression contributes to the progression of OA. Safranin O and Fast Green staining revealed severe joint damage in *Optn*-knockout mice. Additionally, Osteoarthritis Research Society International (OARSI) scores in the medial femoral condyle (MFC) and medial tibial plateau (MTP) were significantly higher in *Optn*-knockout mice than those in the wild-type control mice (Fig. 2a, f, g). Immunohistochemical staining showed a significant reduction in the extracellular matrix components, collagen II (Fig. 2b, h) and aggrecan (Fig. 2c, i), in the cartilage of *Optn*-knockout mice. In contrast, enzyme matrix metalloproteinase 13 (MMP13) and ADAM metalloproteinase with thrombospondin type 1 motif 5 (ADAMTS5), which mediate extracellular matrix degradation, were significantly upregulated in *Optn*-knockout mice compared with wild-type control mice (Fig. 2d, j, e, k). These findings are consistent with our mass spectrometry results in bone tissues (refer to Supplementary Data 1), which showed a decrease in Collagen II and an increase in MMP13 in *Optn*-knockout mice (Supplementary Fig. 1).

### *Optn*-knockout mice exhibit abnormal mitophagy

Next, we analyzed the effect of OPTN downregulation on mitophagy. Electron microscopy of chondrocytes isolated from *Optn*-knockout mice revealed severe cytoplasmic vacuolization, nuclear condensation, mitochondrial swelling, and decreased and disorganized mitochondrial cristae compared to those isolated from wild-type mice (Supplementary Fig. 2). LC3II/I was decreased in *Optn*-knockout chondrocyte, TOMM20 and

TOMM40 did not have significant change (Supplementary Fig. 3). A reduction in mitochondrial membrane potential was observed during injury, as evidenced by JC-1 staining. TOMM40 staining indicated a significant decrease in the length-to-width ratio and an increase in mitochondrial fragmentation in *Optn*-knockout chondrocytes compared to those in wild-type control chondrocytes (Fig. 3a). The mitochondrial permeability transition pore (mPTP) assay, which detects the open state of mitochondrial membrane channel proteins, showed a clear decrease in green fluorescence in the mitochondria of *Optn*-knockout chondrocytes, indicating increased opening of membrane channel proteins (Fig. 3b).

Additionally, the findings revealed an increased monomer/aggregate ratio and a higher proportion of damaged mitochondria in *Optn*-knockout chondrocytes than those in normal chondrocytes (Fig. 3c). Lentivirus-mediated overexpression of OPTN in chondrocytes resulted in reduced intracellular reactive oxygen species (ROS) levels, as detected by 2',7'-dichlorodihydrofluorescein diacetate staining (Supplementary Fig. 4). Fluorescent colocalization of MitoTracker and LC3 was significantly reduced in *Optn*-knockout chondrocytes, indicating a significant reduction in mitophagy levels and accumulation of damaged mitochondria (Fig. 3d).

Next, we investigated the effects of mitophagy dysfunction on chondrocytes using senescence-associated  $\beta$ -galactosidase (SA- $\beta$ -gal) staining. The analysis revealed a significantly higher positive staining of  $\beta$ -galactosidase in *Optn*-knockout chondrocytes than that in the control chondrocytes (Fig. 4a, d), and western blot analysis detected an increase in the expression of the aging marker rH2AX (Supplementary Fig. 1). These results suggest a senescent phenotype in *Optn*-knockout chondrocytes. Caspase 3 staining indicated an increase in apoptosis in *Optn*-knockout chondrocytes (Fig. 4b, e), while Annexin5/PI staining showed a significant increase in double-positive Annexin5/PI cells (Fig. 4c).

### *Optn*-knockout mice exhibit abnormal cartilage development and significant OA symptoms

To investigate the impact of *Optn*-knockout on chondrocyte apoptosis and its effect on mouse articular cartilage development, we conducted a micro-CT analysis of the tibial plateau of *Optn*-knockout mice. The cartilage interface, Tb.BV/TV, Tb.Th, and Tb.N of the subchondral bone were increased in *Optn*-knockout mice, indicating a clear phenotype of OA (Fig. 5a–e). Additionally, we performed corresponding behavioral tests. The von Frey test revealed a decreased pain threshold in *Optn*-knockout mice, the rotarod test demonstrated impaired motor ability, the balance beam test confirmed reduced balance ability, and the footprint test indicated altered gait compared to the control group (Fig. 5f–n). These findings suggest that *Optn*-knockout affects chondrocyte development, resulting in the manifestation of OA phenotype in mice.

### Fasting promotes the expression of OPTN and alleviates OA symptoms

Next, we investigated the effects of calorie restriction on OPTN-mediated mitophagy and OA by subjecting the surgical destabilization of the medial meniscus (DMM) model of OA to a calorie restriction regimen. The results showed that calorie restriction stimulated the expression of OPTN, as indicated by immunohistochemical analysis of the cartilage tissue, which showed upregulation of OPTN in the Fasting + DMM group compared to that in the DMM group (Fig. 6h, l). Micro-CT analysis revealed decreased Tb.BV/TV, Tb.Th, and Tb.N in the subchondral bone of the Fasting+DMM group compared to those in the DMM group, partially alleviating the OA phenotype (Fig. 6a–e). Safranin O and Fast Green staining revealed ameliorated joint damage in the Fasting + DMM group, with significantly lower OARSI scores in the MFC and MTP than those in the DMM group (Fig. 6f, i, j). Furthermore, the extracellular matrix Collagen II level was higher in the Fasting + DMM group than that in the DMM group (Fig. 6g, k). Behavioral tests also demonstrated an increased pain threshold and improved motor ability, gait, and balance in the Fasting + DMM group compared to those

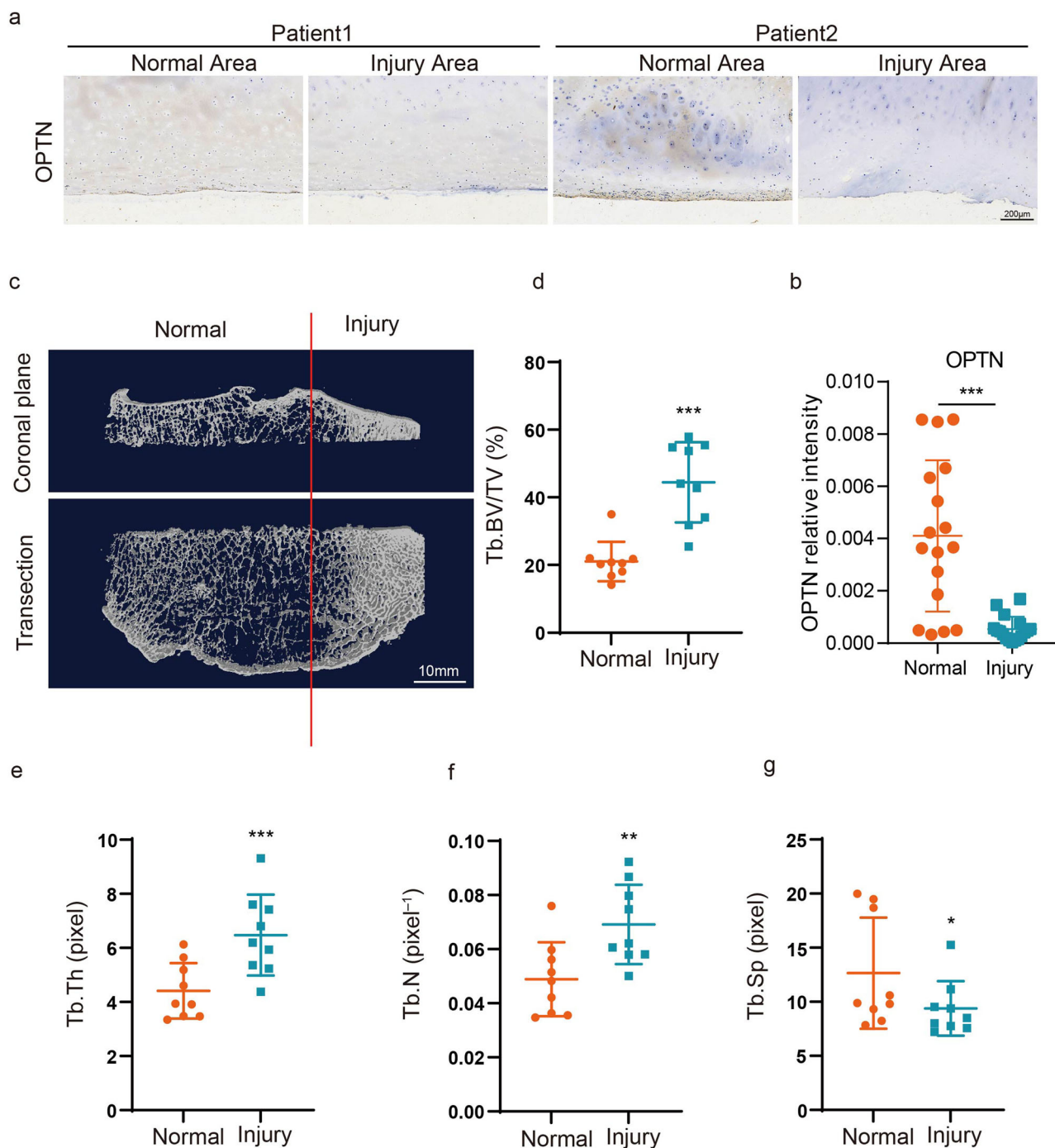


**Fig. 1 | Optineurin (OPTN) is downregulated in the damaged cartilage of patients with osteoarthritis.** **a** Representative immunohistochemical staining of images of normal and damaged cartilage tissues isolated from patients with OA ( $n = 17$ ). **b** OPTN expression level in knee joint cartilage tissues obtained from patients with OA;  $n = 17$ ; Data represent the mean  $\pm$  standard error of means (SEM),  $***p < 0.001$ , unpaired  $t$ -test. **c** Three-dimensional reconstruction images of the tibial plateau from patients with OA analyzed using micro-computed tomography.

Left: Normal side; Right: Damaged side; Top: Coronal plane; Bottom: Transsection. Statistical analysis of bone parameters, including **d** bone volume fraction (Tb.BV/TV), **e** trabecular thickness (Tb.Th), **f** trabecular number (Tb.N), and **g** trabecular separation (Tb.Sp) in normal and damaged cartilage tissue samples isolated from patients with OA quantified using CTAn v1.9 software. Data represent the mean  $\pm$  SEM,  $*p < 0.05$ ,  $**p < 0.01$ ,  $***p < 0.001$ .

in the DMM group, indicating that calorie restriction can alleviate OA symptoms by stimulating OPTN expression (Supplementary Fig. 5).

### Discussion

In this study, we demonstrated that the autophagy receptor OPTN has the potential to alleviate OA symptoms and elucidated the key molecules involved in the influence of mitophagy on OA development. We also

discovered that dietary intervention effectively alleviated OA symptoms by promoting OPTN-mediated mitophagy, thereby providing new insights and targets for the treatment of OA.

Studies have shown that mitophagy, the process by which cells selectively degrade damaged mitochondria, plays a critical regulatory role in OA pathogenesis. However, the specific mechanisms by which mitophagy regulates OA remain unclear. Most studies suggest that the promotion of

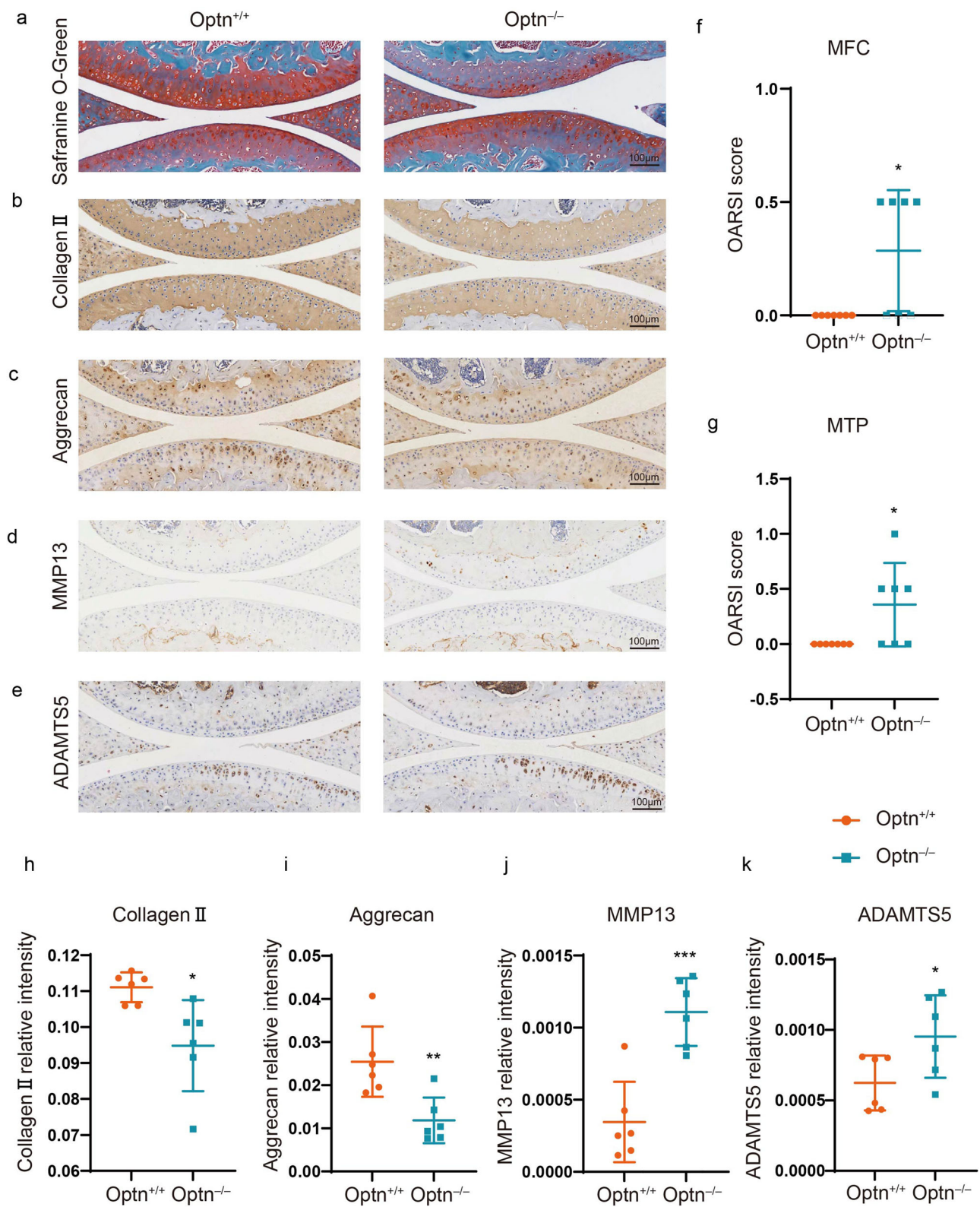


**Fig. 2 | Global knockout of *Optn* induces an osteoarthritis-like phenotype.**  
**a** Representative images of Safranin O-fast green staining showing joint surface erosion in *Optn*-knockout (*Optn*<sup>-/-</sup>) mice. Representative images of immunohistochemical staining for analysis of the expression of collagen II (**b**), Aggrecan (**c**), MMP13 (**d**), and ADAMTS5 (**e**) in (*Optn*<sup>-/-</sup>) and wild-type mice (*Optn*<sup>+/+</sup>) mice.

OARSI scores in the **f** medial femoral condyle (MFC) and **g** medial tibial plateau (MTP) of the *Optn*<sup>-/-</sup> and *Optn*<sup>+/+</sup> mice. Quantification of immunohistochemical staining data: **h** collagen II, **i** aggrecan, **j** MMP13, and **k** ADAMTS5 in *Optn*<sup>-/-</sup> and *Optn*<sup>+/+</sup> mice. Data are presented as the mean ± SEM (unpaired *t*-test, \**p* < 0.05, \*\*\**p* < 0.001; *n* = 6).

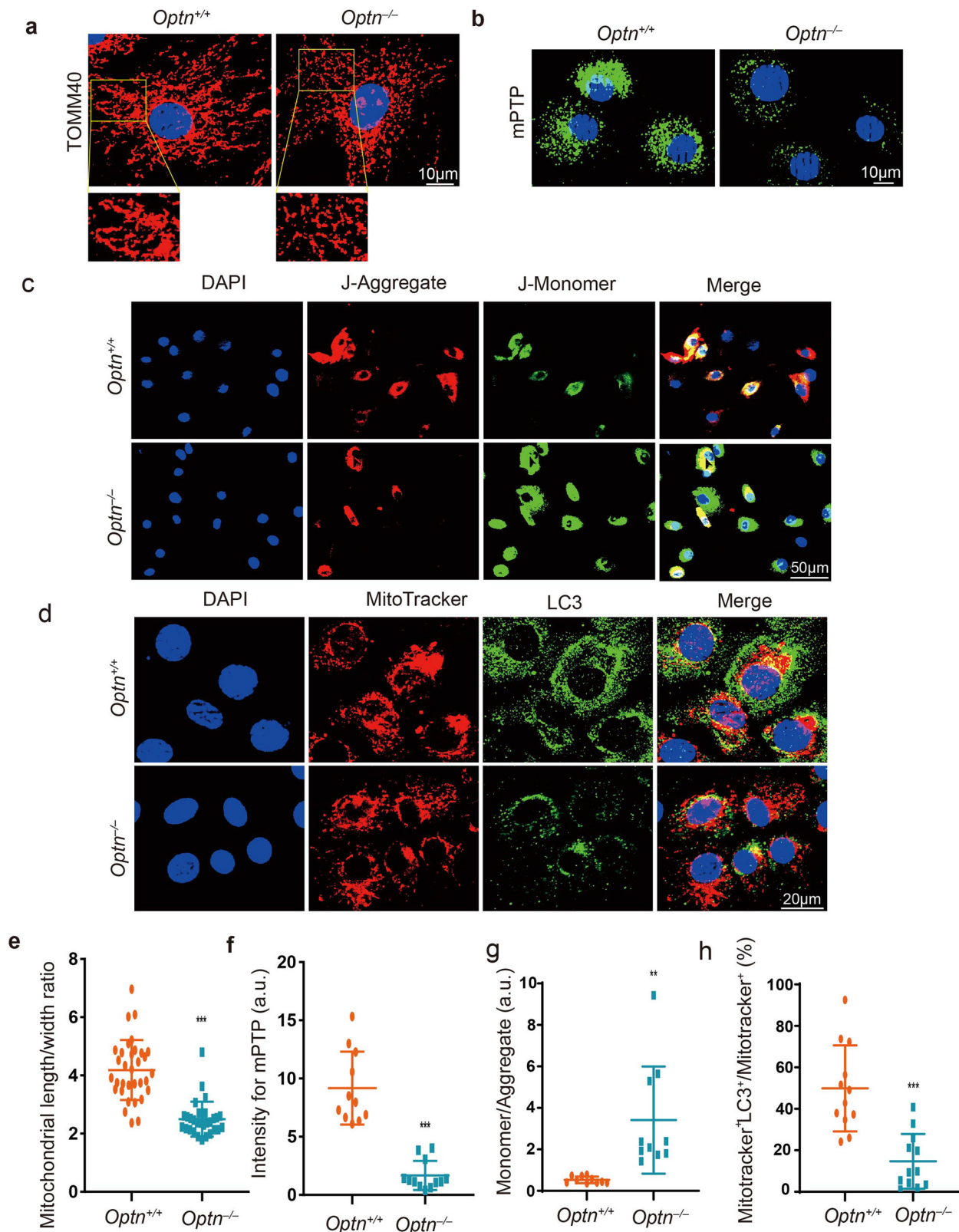


**Fig. 3 | Depletion of OPTN in mice causes the disorder of mitophagy.**

**a** Immunofluorescence staining of TOMM40 shows a decrease in the length-to-width ratio of mitochondria, suggesting an increase in fragmentation in chondrocytes of *Optn*-knockout (*Optn*<sup>-/-</sup>) mice. **b** Enhanced opening of mitochondrial membrane channels was observed in chondrocytes of *Optn*<sup>-/-</sup> mice as evidenced by a reduction in green fluorescence retention within the mitochondria. This indicates an

increased degree of mPTP opening. **c** JC-1 staining shows an increased ratio of monomer/aggregate in chondrocytes of *Optn*<sup>-/-</sup> mice, indicating a decrease in mitochondrial membrane potential. **d** Decreased co-localization of MitoTracker and LC3 show suppressed autophagy in chondrocytes of *Optn*<sup>-/-</sup> mice. **e–h** Statistical analysis of quantified data shown in (a–d). Data show the mean ± SEM; Unpaired *t*-test, \*\**p* < 0.01, \*\*\**p* < 0.001; *n* = 33, 11, 10, and 12 in (a–d), respectively.

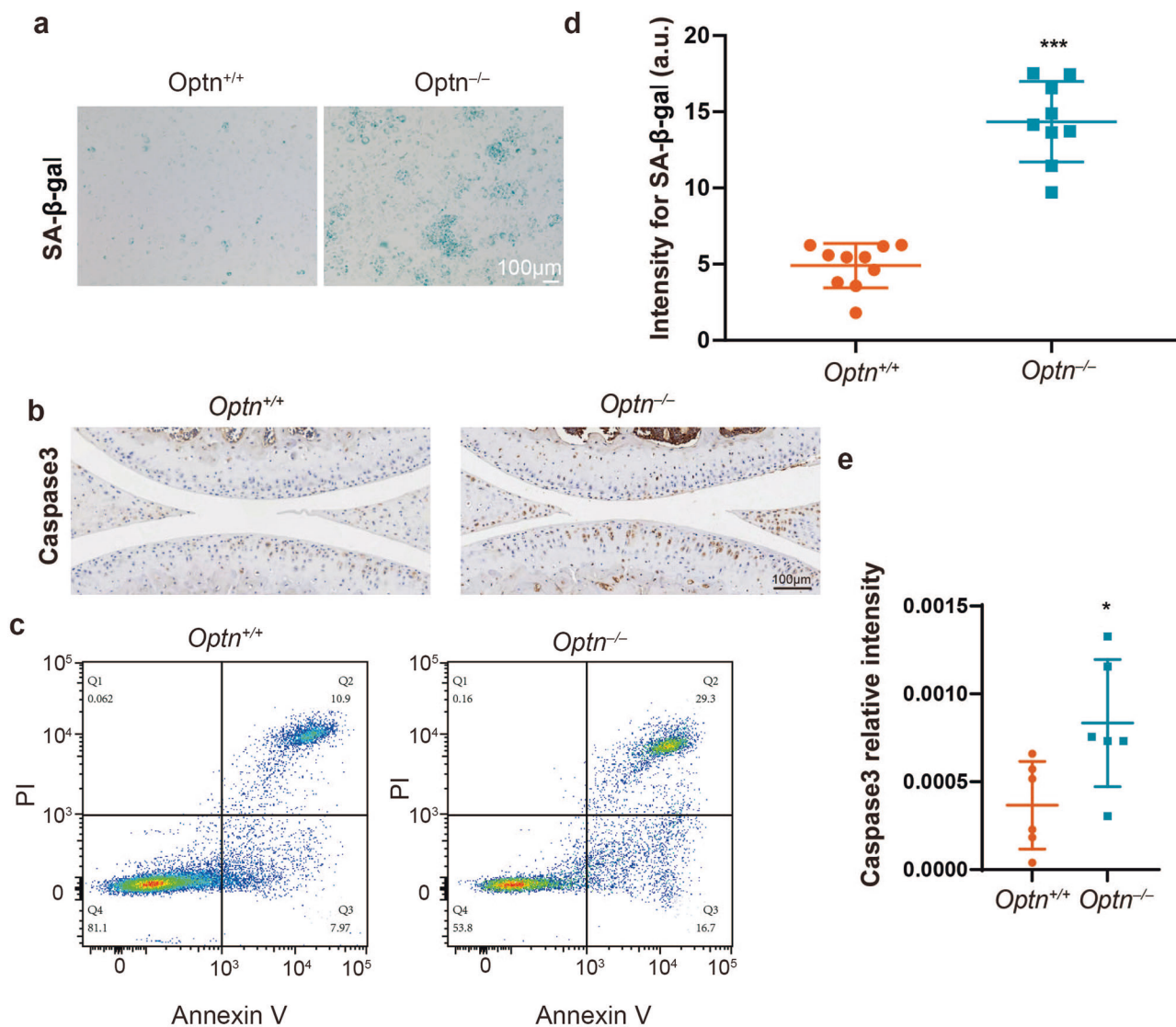


**Fig. 4 | Depletion of OPTN results in chondrocyte apoptosis caused by impaired mitophagy.** Representative images show increased **a** senescence-associated β-galactosidase (SA-β-gal), **b** Caspase3 staining in chondrocytes from *Optn*-knockout (*Optn*<sup>-/-</sup>) mice, **c** Flow cytometry and Annexin V/PI staining show cell apoptosis of

chondrocytes. **d, e** Statistical analysis of the quantified results of images in (a, b). Data represent the mean ± SEM (unpaired *t*-test, \**p* < 0.05, \*\*\**p* < 0.001; *n* = 10 and 6 in (a, b), respectively).

mitophagy can inhibit OA progression. For example, changes in gene expression, such as *A2AR* knockout<sup>14</sup>, *Lpr1* knockout<sup>15</sup>, decreased *LONPI* expression<sup>16</sup>, and *PHF23* overexpression<sup>17</sup>, have been linked to insufficient mitophagy, thereby promoting OA progression. Conversely, drugs such as metformin<sup>7</sup>, 17β estradiol<sup>18</sup>, dimethylxalylglycine<sup>19</sup>, and bone marrow mesenchymal stem cell-derived exosomes<sup>20</sup> have been shown to enhance mitophagy and thereby alleviate OA. However, some studies have indicated that the activation of mitophagy promotes OA progression<sup>21–23</sup>. For instance, inhibiting mitophagy in C28/I2, a normal human chondrocyte cell line, leads to reduced HIF1A expression, promoting cell death, and an OA-like phenotype<sup>21</sup>. Similarly, *Pgc1a* knockout in mice increases mitophagy, exacerbating OA<sup>22</sup>, whereas gubitong (GBT) inhibits mitophagy, thereby suppressing OA<sup>23</sup>. This discrepancy in the results may stem from the failure to distinguish between the two different outcomes of mitophagy: one where mitophagy is adaptively activated to clear damaged mitochondria, and the other where damaged mitochondria accumulate due to ineffective clearance.

Our study revealed that defects in the autophagy receptor protein OPTN, which is involved in mitophagy, led to the accumulation of damaged mitochondria and impaired mitophagy. This resulted in ineffective

clearance of damaged mitochondria and exacerbation of the OA phenotype. These findings provide a deeper understanding of the molecular basis of mitophagy. In particular, we found that TOMM20 and TOMM40, established indicators of mitochondrial mass, did not show a significant change in *Optn* knockout mice. Although mitochondrial mass is influenced by both mitophagy and mitochondrial biogenesis, it does not directly reflect mitophagy activity. Consequently, dysfunctional mitochondria may accumulate in *Optn* knockout chondrocytes, while a corresponding decrease in mitochondrial biogenesis could maintain the overall mitochondrial mass. Furthermore, fluctuations in mitochondrial number can result from dynamic fusion and fission events. Overall, there is no significant change in mitochondrial mass when the *Optn* gene is knocked out. A precise understanding of the molecular mechanisms of OPTN-mediated mitophagy needs further in-depth studies. Future studies should focus on the identification of its binding partner in the mitochondria and investigate the protein interactions that occur during mitophagy, particularly those involving ubiquitinated outer mitochondrial membrane proteins.

Fasting can alleviate OA and promote mitochondrial homeostasis<sup>11,12</sup>. Consistent with these findings, we also showed that fasting can activate OPTN-mediated autophagy, leading to reduced mitochondrial damage and

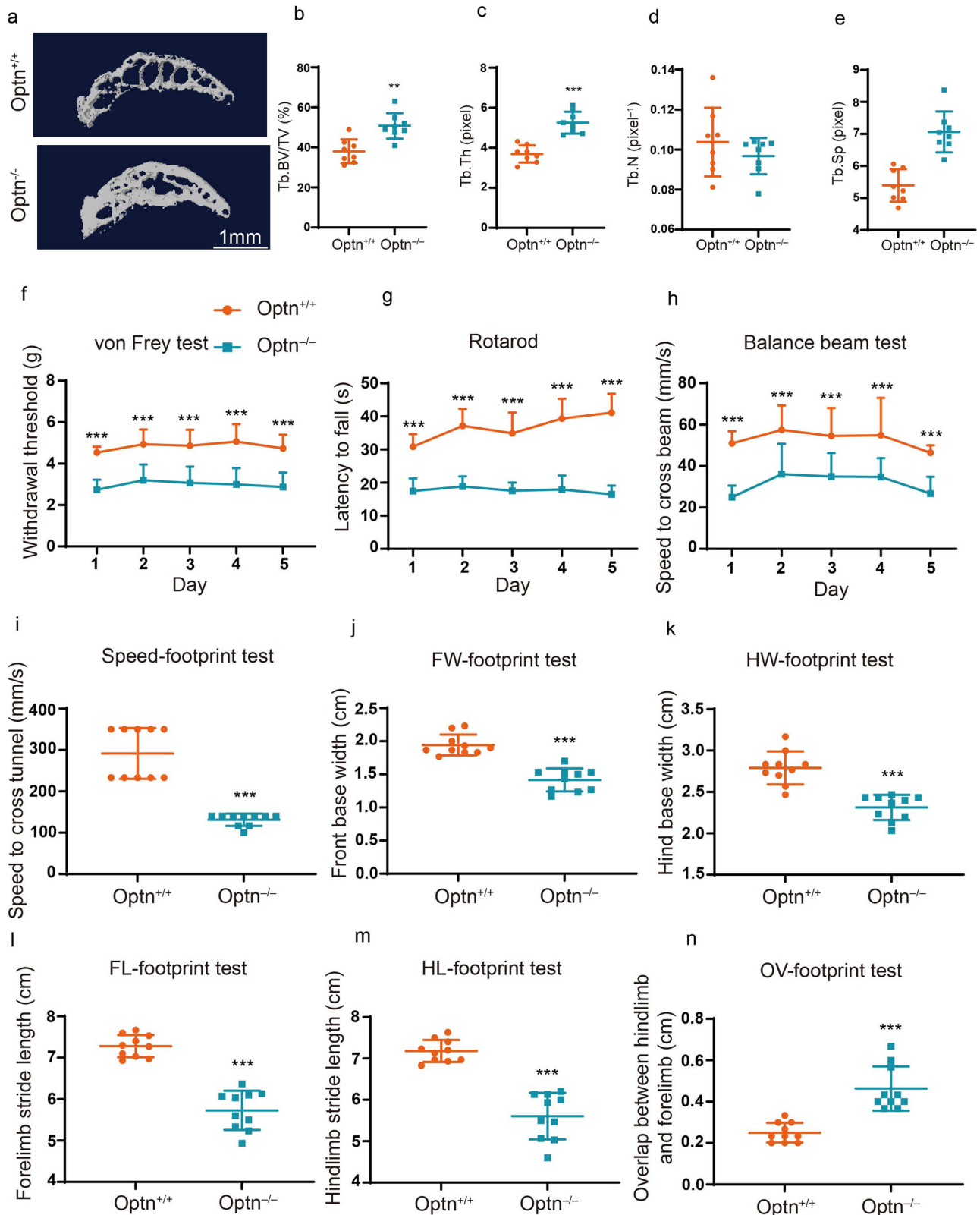


**Fig. 5 | Depletion of OPTN results in OA-like phenotypes.** **a** Three-dimensional reconstruction images of the tibial plateau analyzed using micro-CT. Statistical analysis of bone parameters, including **b** bone volume fraction (Tb.BV/TV), **c** trabecular thickness (Tb.Th), **d** trabecular number (Tb.N), and **e** trabecular

separation (Tb.Sp). Pain perception, limb strength, balance ability, and gait of the animal assessed using **f** von Frey, **g** rotarod, **h** balance beam, and **i–n** footprint tests, respectively. Data represent the mean ± SEM (two-way ANOVA for **f–h**) and unpaired *t*-test for **(a–e)** and **(i–n)**, \*\*\**p* < 0.001; *n* = 10).

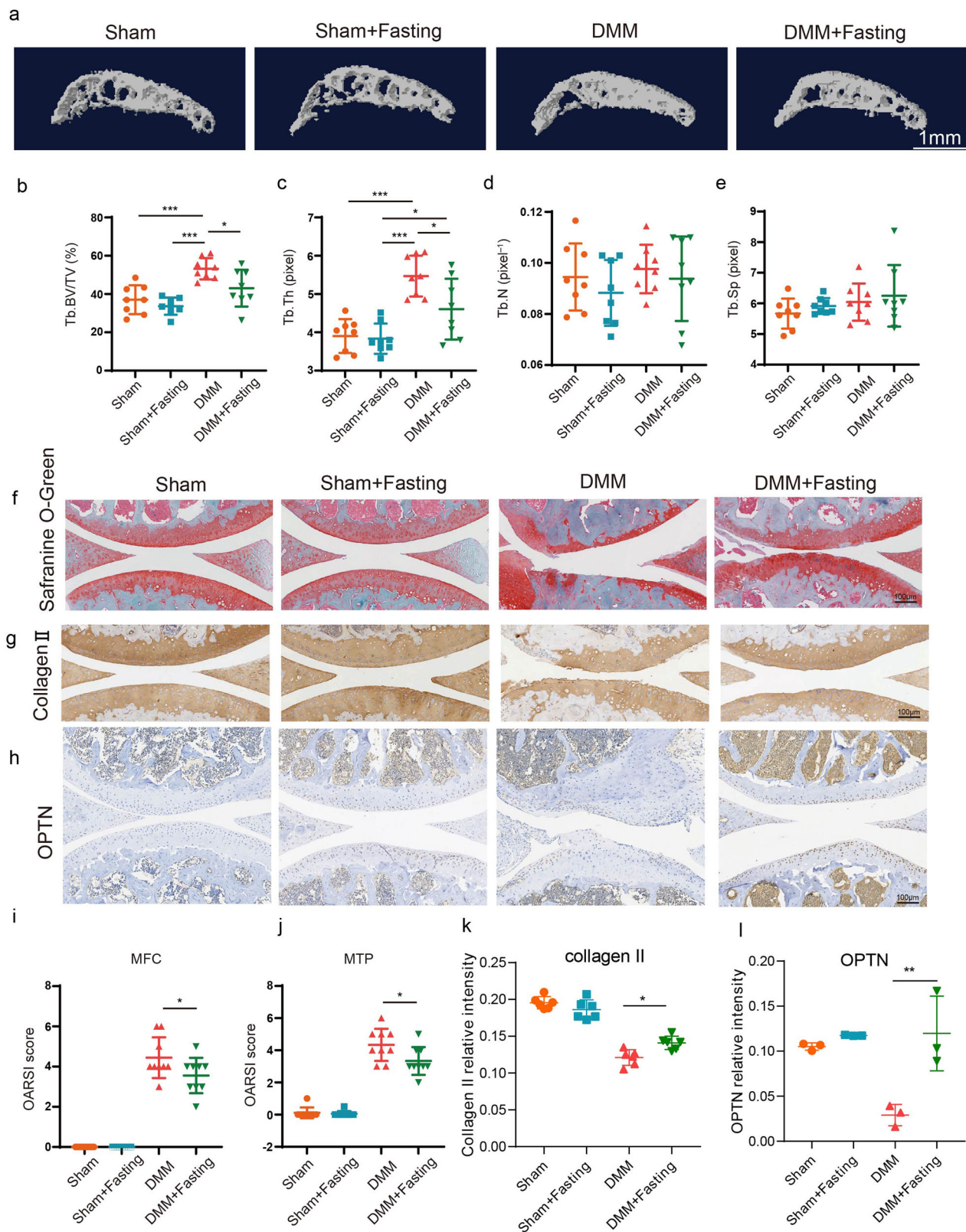
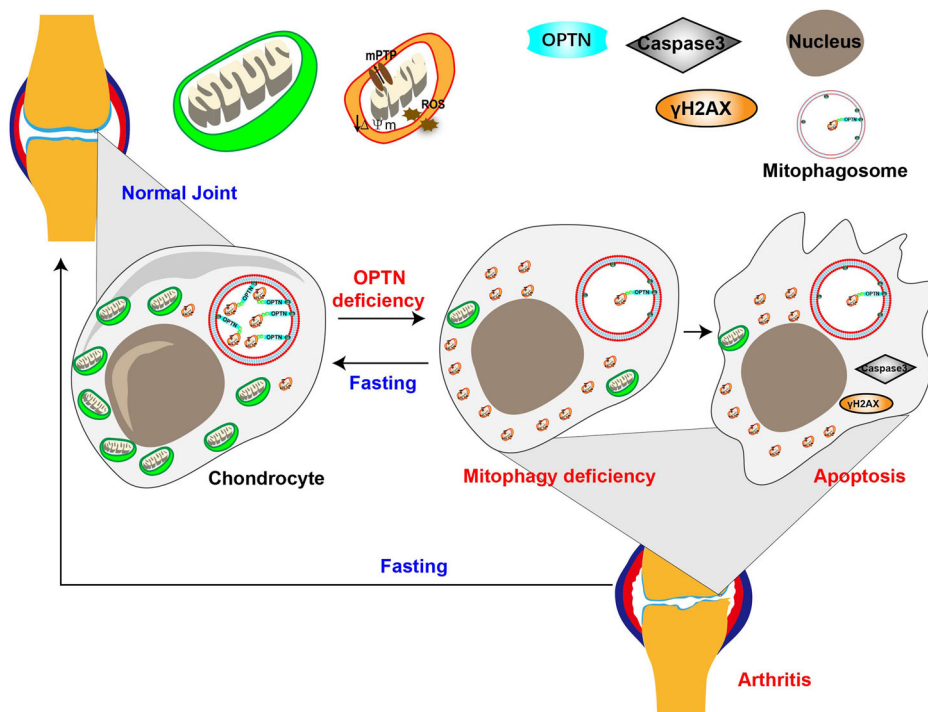


**Fig. 6 | Fasting activates OPTN-mediated mitophagy in chondrocytes to protect against osteoarthritis.** **a** Three-dimensional reconstruction images of the tibial plateau analyzed using micro-CT imaging. Statistical analysis of bone parameters, including **b** bone volume fraction (Tb.BV/TV), **c** trabecular thickness (Tb.Th), **d** trabecular number (Tb.N), and **e** trabecular separation (Tb.Sp). **f** Representative images of Safranin O-fast green staining show joint surface erosion.

**g, h** Representative images of immunohistochemistry show expression of extracellular matrix proteins collagen II and OPTN in DMM mice upon fasting treatment. **i-l** Statistical analysis of the quantified results shown in (f, g), showing OARSJ scores and protein expression levels of collagen II and OPTN in the medial femur condyle (MFC) and medial tibial plateau (MTP). Data are presented as the mean  $\pm$  SEM (unpaired *t*-test, \**p* < 0.05, \*\*\**p* < 0.001; *n* = 6).

**Fig. 7 | Schematic illustration demonstrating fasting alleviates osteoarthritis by activating OPTN-mediated mitophagy.** Defects in the autophagy receptor OPTN in chondrocytes lead to insufficient mitophagy, accumulation of damaged mitochondria, and chondrocyte apoptosis, which are important causes of articular cartilage damage. Fasting alleviates the occurrence of osteoarthritis by activating OPTN-mediated mitophagy.



alleviated OA symptoms. However, the precise mechanisms underlying the effects of fasting on the alleviation of OA remain unclear. Therefore, further studies are essential to validate the activation of OPTN-mediated mitophagy through dietary intervention in populations with OA.

In conclusion, our results demonstrated that *Optn*-knockout mice exhibited accumulated dysfunctional mitochondria and aberrant mitophagy, leading to chondrocyte apoptosis and OA progression (Fig. 7). We also showed that fasting activated OPTN-mediated autophagy, leading to the alleviation of OA symptoms, suggesting that OPTN plays a crucial role in mitigating OA progression. These findings highlight the potential of OPTN as a therapeutic target for OA. Nevertheless, future studies are required to validate these findings by either overexpressing or inhibiting the degradation of OPTN to confirm its efficacy in reducing OA progression.

## Materials and methods

### Animal handling and ethical approval

*Optn*-knockout mice (*Optn*<sup>tm1a</sup>/EUCOMM)<sup>Wtsi</sup>; MASV; EPD0116\_2\_G06) were generated as part of the European Conditional Mouse Mutagenesis Program (EUCOMM). The animal experiments conducted in this study followed the animal welfare guidelines set by the World Organization for Animal Health and the Chinese National Animal Experimentation Guidelines. Twelve-month-old male mice were used in this study.

All study participants provided informed consent. All animal and human studies were approved by the Ethical Review Board of Xiangya Hospital of Central South University (approval no. 2019121189, 202103626).

### Mouse DMM OA model

DMM surgery was performed on the left knee joints of mice, as previously described<sup>24</sup>. Briefly, 8-week-old male C57BL/6 mice (weighing 18–25 g) obtained from the SLRC Laboratory Animal Center were randomly assigned to DMM or sham groups. Mice were anesthetized using Avertin (350 μL/20 g) [1.25% (w/v) 2,2,2-tribromoethyl alcohol (Avertin) was dissolved in 10 mL tert-amyl alcohol, and the final volume was adjusted to 400 mL using saline], and subjected to medial arthrotomy of the left knee. In the DMM group, the medial meniscotibial ligament of the left joint was exposed and transected using micro-iris scissors. Control mice were subjected to medial arthrotomy of the left knee without severing the medial

meniscotibial ligament. After surgery, mice were monitored daily for the first week and three times per week during the study period for signs of physical distress.

### Intermittent fasting

The experimental animal fasting protocol was performed according to a previously described method<sup>25</sup>. The mice were fasted for 24 h thrice a week (on days 2, 4, and 6), followed by ad libitum re-feeding of a standard solid diet for 1 week. This fasting-refeeding cycle was repeated for 2 months.

### Knee joint procurement

The mice were euthanized by decapitation, and their knee joints were promptly extracted. The joints were post-fixed in 4% paraformaldehyde for 48 h at 4 °C. For paraffin sectioning, the joints were decalcified in 14% ethylenediaminetetraacetic acid (EDTA; pH 7.4) for 7 days. Alternatively, frozen sections of the joints were cryoprotected using 35% sucrose.

### Isolation of primary mouse chondrocytes

After euthanization by cervical dislocation, the body surfaces of the mice were sterilized with 70% ethanol. Articular cartilage tissue was dissected and chopped into small fragments (approximately 1–2 mm in size). The cartilage fragments were transferred into a centrifuge tube containing collagenase solution prepared in DMEM/F-12 (typically 0.2–0.25% collagenase type II). The tubes were then incubated at 37 °C for 2–4 h with gentle agitation. Afterward, the cells were separated from the undigested tissue fragments for a few minutes, and the cell-rich supernatant was collected without disturbing the pellet. The cell suspension was centrifuged at 300 × g for 5 min to pellet chondrocytes. The supernatant was discarded, and the cell pellet was resuspended in DMEM/F-12 supplemented with 10% FBS and 1% penicillin-streptomycin solution. The culture medium was changed every 2–3 days and cell growth and morphology were monitored under a microscope. Isolated mouse chondrocytes were used for further downstream experiments.

### SA-β-gal staining

SA-β-gal staining, which detects β-galactosidase activity, was used to investigate cellular senescence. Briefly, cells were fixed in 4% PFA for 15 min and then incubated in staining buffer (0.1 M citric acid and sodium

phosphate, pH 6.0) at 37 °C for 4 h, followed by incubation with the staining substrate (5 mM X-gal and 5 mM potassium ferrocyanide in 40 mM citric acid/sodium phosphate buffer, pH 6.0) at 37 °C in a dark humidified chamber. The staining results were analyzed using a microscope.

### Micro-CT analysis

Knee joints from mice were fixed in 4% paraformaldehyde for 48 h and then examined using high-resolution micro-CT (VIVACT 80; SCANCO Medical AG, Switzerland) following established protocols. The scanner settings were adjusted to 55 kV and 145  $\mu$ A, with a resolution of 11.4  $\mu$ m. Image reconstruction software (NRecon), data analysis software (CTAn v1.9), and three-dimensional model visualization software (micro-CT Vol v2.0) were used to analyze the tibial subchondral bone. A three-dimensional histomorphometric analysis was performed using longitudinal images of the tibial subchondral bone. The region of interest (ROI) encompassed the entire medial compartment of the subchondral bone. Trabecular bone parameters, including Tb.BV/TV, Tb.Th, Tb.N, and Tb.Sp were measured.

### Immunohistochemistry

The knee joints of mice were harvested. For sectioning, bones were embedded in paraffin. Immunostaining was performed according to a standard protocol. The sections were incubated with antibodies against Collagen II (Thermo Fisher, PA5-79057; 1:100), aggrecan (Abcam, ab36861; 1:100), MMP13 (ZEN-BIOSCIENCE, 820098; 1:100), ADAMTS5 (GeneTex, GTX100332; 1:50), OPTN (Proteintech, 10837-1-AP; 1:50), and Caspase3 (Thermo Fisher, 700182; 1:50). A horseradish peroxidase–streptavidin detection kit (Dako) was used for immunohistochemical staining to detect immunoreactivity, followed by counterstaining with hematoxylin (Dako, S3309). The paraffin sections were stained with Safranin O–fast Green (Millipore). Images were acquired using a microscope (Olympus, CX31; Japan).

### Mitophagy and quality control of mitochondria

We performed co-staining with MitoTracker and LC3 to analyze the mitophagic activity. JC-1 staining was conducted to assess mitochondrial membrane potential, and the monomer (green)/aggregate (red) ratio was calculated (green indicates low membrane potential, whereas red indicates high membrane potential)<sup>26</sup>. TOMM40 staining was used to evaluate the degree of mitochondrial fragmentation by calculating the aspect ratio of the mitochondria. The extent of mitochondrial membrane channel opening was determined by measuring the residual green fluorescence of mPTP-stained cells. Intracellular reactive oxygen species levels were determined using a Reactive Oxygen Species assay kit. The following reagents were used: JC-1 staining kit (Beyotime, C2006), Reactive Oxygen Species assay kit (Solarbio, CA1410), TOMM40 (Proteintech, 18409-1-AP), MitoTracker (Beyotime, C1035), and LC3B antibody (Sigma-Aldrich, L7543). Mitochondrial Permeability Transition Pore Assay Kit or mPTP Assay Kit (Beyotime, C2009S). The rationale of this experiment as following: Cells were first stained with Calcein AM and subsequently treated with cobalt chloride (containing  $\text{Co}^{2+}$ ). Under normal conditions, Calcein emits green fluorescence. Following exposure to  $\text{Co}^{2+}$ , it forms calcein- $2\text{Co}^{2+}$  complexes, which are non-fluorescent. Although  $\text{Co}^{2+}$  alone cannot diffuse into mitochondria, mitochondrial dysfunction can induce opening of the mitochondrial permeability transition pore (mPTP), permitting  $\text{Co}^{2+}$  entry and thereby quenching the green fluorescence. Consequently, a stronger green fluorescence signal corresponds to a lower degree of mPTP opening.

For the colocalization of MitoTracker and LC3, chondrocytes were incubated with MitoTracker (200 nM) for 30 min at 37 °C. After washing with PBS, the chondrocytes were fixed and then incubated with an LC3B antibody, followed by FITC-conjugated donkey anti-rabbit secondary antibody. Images were captured using a fluorescence microscope.

### OARSI scoring

Histopathological assessments were based on the OARSI grading system<sup>27</sup>. The grade was defined as the OA depth progression into the cartilage (grade 0, surface intact; cartilage morphology intact; grade 1, surface intact; grade 2,

surface discontinuity; grade 3, vertical fissures; grade 4, erosion; grade 5, denudation; and grade 6, deformation). OA stage represents the proportion of the articular surface that is involved in OA compared to the total surface length (stage 0, no OA activity; stage 1, <10%; stage 2, 10–25%; stage 3, 25–50%; stage 4, >50%). For OA, lesion depth in the cartilage area (grade) represents more severe arthritis, and lesion extent over the cartilage surface (stage) represents the extent of the disease. The semiquantitative OARSI score was calculated as follows: OARSI score = grade  $\times$  stage.

### von Frey testing

The mechanical allodynia test of the hind limb was performed using von Frey filaments (IITC, Woodland Hills, CA, USA), as previously described<sup>28</sup>. Briefly, mice were allowed to acclimatize for 15 min in plastic cages with a wire mesh bottom. A von Frey filament (typical force range used in mice is 0.4 to 6.0 g) was applied perpendicularly to the plantar surface of the hind paw until it just bent and then held in place for 3 s. If the mouse withdrew, licked, or shook its paw, a positive response was reported and the von Frey threshold (g) was recorded. An up-down iterative method was used to determine withdrawal thresholds. The tests were performed in a blinded manner, and the investigator was not aware of the identification of the animals or study groups.

### Rotarod test

Motor coordination and balance were assessed using the accelerating rotarod test with slight modifications<sup>29</sup>. Mice were positioned on a rubber surface rod (36 mm in diameter) of an accelerating rotarod apparatus (DXP-3; Chinese Academy of Medical Sciences). The rod was initially rotated at a velocity of 1 cm/s and then accelerated at a rate of 1.75 rpm/s. The time taken by the mouse to fall from the rod was recorded as the latency to fall. Each mouse underwent one session per day, with three trials conducted at 20-min intervals for a total of five consecutive days.

### Footprint test

The footprint test, as previously described<sup>29</sup>, was used to analyze the gait of the mice. A non-toxic waterproof paint was used to coat the paws of the mice—red-colored paint was applied to the forepaws and black-colored paint was applied to the hind paws. The mice were then placed at one end of a straight and narrow tunnel (10  $\times$  10  $\times$  70 cm) with white paper lining the bottom to capture the footprints. Each mouse was subjected to the following steps: the recorded parameters included front base width, hind base width, forelimb stride length, hindlimb stride length, overlap between the hindlimb and forelimb, and crossing speed through the tunnel.

### Balance beam test

Balance maintenance was assessed by using a modified version of a previously described method<sup>29</sup>. The mice were positioned at one end of a wooden bar (0.9 cm  $\times$  0.9 cm  $\times$  50 cm) suspended 40 cm above the ground. A cage was placed beneath the bar and a dark goal box was positioned at the other end to incentivize the mouse to run in a safe and dark environment. The time required for the mice to traverse the beam was recorded and the crossing speed was calculated. Each mouse underwent three trials per day, with a 20-min interval between each trial for five consecutive days.

### Mass spectrometric analysis

Mass spectrometry (MS) was conducted using proteins extracted from mouse bone tissue. The basic MS analysis data has been provided in an Excel file as Supplementary Material. Methods for LC-MS analysis was described in our previous work<sup>10</sup>.

### Transmission electron microscopy

Cartilage tissue was harvested and cut into 1  $\times$  1  $\times$  2 mm<sup>3</sup> fragments. Within 1-min post-excision, the tissue samples were immersed in a 2.5% glutaraldehyde fixative solution. Alternatively, cell pellets were similarly fixed in 2.5% glutaraldehyde. All specimens were then prepared in the Electron Microscopy Facility at Xiangya Hospital, Images are recorded digitally

(Gatan 830P22w44, American) for subsequent analysis of structural details. The aspect ratio of the mitochondria (mitochondrial length/width ratio) was calculated. In Supplementary Fig. 2, each dot corresponds to an individual mitochondrion. Six mitochondria per cell were analyzed, with 5 independent replicates conducted, resulting in a total of 30 mitochondria per group.

### Statistical analysis

The data were analyzed using GraphPad Prism 7 software and are presented as mean  $\pm$  SEM. The unpaired *t*-test was used to compare two groups with one variance. Distribution style was assessed using the Shapiro–Wilk normality test. For multiple comparisons, analysis of variance (ANOVA) was used, with one-way ANOVA for studying single variances and two-way ANOVA for studying multiple variances. Dunnett's multiple comparison test was conducted as a post hoc analysis to determine statistically significant differences between the two groups. In all experiments, a *p* value of  $<0.05$  was considered statistically significant.

### Reporting summary

Further information on research design is available in the Nature Portfolio Reporting Summary linked to this article.

### Data availability

The Source data behind Supplementary Fig. 1a can be found in the Excel file named Supplementary Data 1. Uncropped blots are provided in Supplementary Fig. 6. Other data are available upon request after acceptance.

Received: 8 April 2024; Accepted: 13 January 2025;

Published online: 16 January 2025

### References

1. Yao, Q. et al. Osteoarthritis: pathogenic signaling pathways and therapeutic targets. *Signal. Transduct. Target. Ther.* **8**, 56 (2023).
2. Duong, V., Oo, W. M., Ding, C., Culvenor, A. G. & Hunter, D. J. Evaluation and treatment of knee pain: a review. *JAMA* **330**, 1568–1580 (2023).
3. Yan, J. et al. Autophagic LC3(+) calcified extracellular vesicles initiate cartilage calcification in osteoarthritis. *Sci. Adv.* **8**, eabn1556 (2022).
4. Duan, R., Xie, H. & Liu, Z. Z. The role of autophagy in osteoarthritis. *Front. Cell Dev. Biol.* **8**, 608388 (2020).
5. Vargas, J. N. S., Hamasaki, M., Kawabata, T., Youle, R. J. & Yoshimori, T. The mechanisms and roles of selective autophagy in mammals. *Nat. Rev. Mol. Cell Biol.* **24**, 167–185 (2023).
6. Shin, H. J. et al. Pink1-mediated chondrocytic mitophagy contributes to cartilage degeneration in osteoarthritis. *J. Clin. Med.* **8**, 1849 (2019).
7. Wang, C. et al. Protective effects of metformin against osteoarthritis through upregulation of SIRT3-mediated PINK1/Parkin-dependent mitophagy in primary chondrocytes. *Biosci. Trends* **12**, 605–612 (2019).
8. Fan, D. X., Yang, X. H., Li, Y. N. & Guo, L. 17beta-Estradiol on the expression of G-protein coupled estrogen receptor (GPER/GPR30) mitophagy, and the PI3K/Akt signaling pathway in ATDC5 chondrocytes in vitro. *Med. Sci. Monit.* **24**, 1936–1947 (2018).
9. Lazarou, M. et al. The ubiquitin kinase PINK1 recruits autophagy receptors to induce mitophagy. *Nature* **524**, 309–314 (2015).
10. Liu, Z. Z. et al. Autophagy receptor OPTN (optineurin) regulates mesenchymal stem cell fate and bone-fat balance during aging by clearing FABP3. *Autophagy* **17**, 2766–2782 (2021).
11. Koppold, D. A. et al. Effects of prolonged fasting during inpatient multimodal treatment on pain and functional parameters in knee and hip osteoarthritis: a prospective exploratory observational study. *Nutrients* **15**, 2695 (2023).
12. Weir, H. J. et al. Dietary restriction and AMPK increase lifespan via mitochondrial network and peroxisome remodeling. *Cell Metab.* **26**, 884–896.e885 (2017).

13. Drinda, S. et al. AGE-RAGE interaction does not explain the clinical improvements after therapeutic fasting in osteoarthritis. *Complement. Med. Res.* **25**, 167–172 (2018).
14. Castro, C. M. et al. Adenosine A2A receptor (A2AR) stimulation enhances mitochondrial metabolism and mitigates reactive oxygen species-mediated mitochondrial injury. *FASEB J.* **34**, 5027–5045 (2020).
15. Yan, W. et al. Heterozygous LRP1 deficiency causes developmental dysplasia of the hip by impairing triradiate chondrocytes differentiation due to inhibition of autophagy. *Proc. Natl. Acad. Sci. USA.* **119**, e2203557119 (2022).
16. He, Y. et al. LONP1 downregulation with ageing contributes to osteoarthritis via mitochondrial dysfunction. *Free Radic. Biol. Med.* **191**, 176–190 (2022).
17. Maimaitijuma, T. et al. PHF23 negatively regulates the autophagy of chondrocytes in osteoarthritis. *Life Sci.* **253**, 117750 (2020).
18. Mei, R. et al. 17beta-Estradiol induces mitophagy upregulation to protect chondrocytes via the SIRT1-mediated AMPK/mTOR signaling pathway. *Front. Endocrinol.* **11**, 615250 (2020).
19. Hu, S. et al. Stabilization of HIF-1alpha alleviates osteoarthritis via enhancing mitophagy. *Cell Death Dis.* **11**, 481 (2020).
20. Tang, S. et al. Bone marrow mesenchymal stem cell-derived exosomes inhibit chondrocyte apoptosis and the expression of MMPs by regulating Drp1-mediated mitophagy. *Acta. Histochem.* **123**, 151796 (2021).
21. Lu, J. et al. Hypoxia inducible factor-1 alpha is a regulator of autophagy in osteoarthritic chondrocytes. *Cartilage* **13**, 1030S–1040S (2021).
22. Kim, D., Song, J. & Jin, E. J. BNIP3-dependent mitophagy via PGC1alpha promotes cartilage degradation. *Cells* **10**, 1839 (2021).
23. Yu, X. B. et al. Chondroprotective effects of gubitong recipe via inhibiting excessive mitophagy of chondrocytes. *Evid. Based Complement. Alternat. Med.* **2022**, 8922021 (2022).
24. Su, W. et al. Angiogenesis stimulated by elevated PDGF-BB in subchondral bone contributes to osteoarthritis development. *JCI Insight.* **5**, e135446 (2020).
25. Jordan, S. et al. Dietary intake regulates the circulating inflammatory monocyte pool. *Cell* **178**, 1102–1114.e1117 (2019).
26. Dong, L. et al. Highly hydrated paramagnetic amorphous calcium carbonate nanoclusters as an MRI contrast agent. *Nat. Commun.* **13**, 5088 (2022).
27. Pritzker, K. P. et al. Osteoarthritis cartilage histopathology: grading and staging. *Osteoarthritis Cartilage* **14**, 13–29 (2006).
28. Li, M. et al. Utx regulates the NF- $\kappa$ B signaling pathway of natural stem cells to modulate macrophage migration during spinal cord injury. *J. Neurotrauma.* **38**, 353–364 (2020).
29. Liu, Z. et al. ALS-associated E478G mutation in human OPTN (Optineurin) promotes inflammation and induces neuronal cell death. *Front. Immunol.* **9**, 2647 (2018).

### Acknowledgements

This study was supported by grants from the National Natural Science Foundation of China [grant numbers: 82172502 and 81974127].

### Author contributions

Z.Z.L. made substantial contributions to the conception and design of the study; Z.Z.L., W.B.H., and M.N.Z. were involved in drafting the manuscript or revising it critically for important intellectual content; R.D., C.G.H., G.H.C., M.J.C., and M.N.Z. contributed significantly to the acquisition, analysis, and interpretation of data; D.Z., Z.L.P., and X.W. collected the clinical samples; H.X., H.F.L., and C.Y.C. provided administrative, technical, and material support; Z.Z.L. has full access to all the data in the study and is responsible for the integrity of the data and accuracy of the data analysis.

### Competing interests

The authors declare no competing interests.

### Additional information

**Supplementary information** The online version contains supplementary material available at

<https://doi.org/10.1038/s42003-025-07541-x>.

**Correspondence** and requests for materials should be addressed to Da Zhong, Hui Xie, Wen-Bao Hu or Zheng-Zhao Liu.

**Peer review information** *Communications Biology* thanks the anonymous reviewers for their contribution to the peer review of this work. Primary Handling Editors: Martina Rauner and Mengtan Xing.

**Reprints and permissions information** is available at <http://www.nature.com/reprints>

**Publisher's note** Springer Nature remains neutral with regard to jurisdictional claims in published maps and institutional affiliations.

**Open Access** This article is licensed under a Creative Commons Attribution-NonCommercial-NoDerivatives 4.0 International License, which permits any non-commercial use, sharing, distribution and reproduction in any medium or format, as long as you give appropriate credit to the original author(s) and the source, provide a link to the Creative Commons licence, and indicate if you modified the licensed material. You do not have permission under this licence to share adapted material derived from this article or parts of it. The images or other third party material in this article are included in the article's Creative Commons licence, unless indicated otherwise in a credit line to the material. If material is not included in the article's Creative Commons licence and your intended use is not permitted by statutory regulation or exceeds the permitted use, you will need to obtain permission directly from the copyright holder. To view a copy of this licence, visit <http://creativecommons.org/licenses/by-nc-nd/4.0/>.

© The Author(s) 2025